Monthly Notices
of the
ROYAL ASTRONOMICAL SOCIETY

MNRAS **473,** 345–354 (2018)
Advance Access publication 2017 August 14

doi:10.1093/mnras/stx2077

Transit visibility zones of the Solar system planets

R. Wells,[1]★ K. Poppenhaeger,[1,2] C. A. Watson[1] and R. Heller[3]

[1]*Astrophysics Research Centre, Queen's University Belfast, Belfast BT7 1NN, UK*
[2]*Harvard–Smithsonian Center for Astrophysics, 60 Garden Street, Cambridge, MA 02138, USA*
[3]*Max Planck Institute for Solar System Research, Justus-von-Liebig-Weg 3, 37077 Göttingen, Germany*

Accepted 2017 August 9. Received 2017 August 8; in original form 2017 June 16

ABSTRACT

The detection of thousands of extrasolar planets by the transit method naturally raises the question of whether potential extrasolar observers could detect the transits of the Solar system planets. We present a comprehensive analysis of the regions in the sky from where transit events of the Solar system planets can be detected. We specify how many different Solar system planets can be observed from any given point in the sky, and find the maximum number to be three. We report the probabilities of a randomly positioned external observer to be able to observe single and multiple Solar system planet transits; specifically, we find a probability of 2.518 per cent to be able to observe at least one transiting planet, 0.229 per cent for at least two transiting planets, and 0.027 per cent for three transiting planets. We identify 68 known exoplanets that have a favourable geometric perspective to allow transit detections in the Solar system and we show how the ongoing *K2* mission will extend this list. We use occurrence rates of exoplanets to estimate that there are 3.2 ± 1.2 and $6.6^{+1.3}_{-0.8}$ temperate Earth-sized planets orbiting GK and M dwarf stars brighter than $V = 13$ and 16, respectively, that are located in the Earth's transit zone.

Key words: extraterrestrial intelligence – astrobiology – planets and satellites: detection – planets and satellites: general.

1 INTRODUCTION

Over the past decade, the number of known of exoplanets has grown immensely. Over 3500 exoplanets have been discovered to date,[1] going from close-orbiting, Jupiter-sized planets (hot Jupiters) to those similar to Earth in mass and size, for example, Kepler-78b (Pepe et al. 2013). A number of temperate extrasolar planets have now been discovered (Vogt et al. 2010; Anglada-Escudé et al. 2013; Jenkins et al. 2015), including one around our nearest neighbour, Proxima Centauri (Anglada-Escudé et al. 2016).

The habitable zone (HZ) is defined as the region around a star where a terrestrial planet could sustain liquid water. It largely depends on the stellar flux received and surface atmospheric pressure, along with other planetary and stellar parameters (Kasting, Whitmire & Reynolds 1993; Kopparapu et al. 2013). That said, planets and even moons beyond the HZ could still have temperate regions, for example, if they are subject to tidal heating (Reynolds, McKay & Kasting 1987; Barnes & Heller 2013). Dressing & Charbonneau (2015) found the occurrence rate of Earth-sized (0.5–$1.4R_\oplus$) planets within the HZ around M-dwarfs to be $0.68^{+0.13}_{-0.08}$ planets per star, while Petigura, Howard & Marcy (2013) found that 22 ± 8 per cent of GK stars harbour slightly larger planets (1–$2R_\oplus$) in their HZ. These values were calculated with the HZ defined as the region around the star, which receives between 0.25 and 4 times the incident stellar flux of Earth. The 39[2] potentially habitable planets discovered thus far plus the expected yield of the *PLATO* mission (Rauer et al. 2014) naturally makes us wonder whether, in fact, some of these worlds could be inhabited, possibly even by intelligent beings.

The vast majority of exoplanets are currently detected through transits. Conversely, one can ask the question where in the Milky Way the transits of the Solar system planets can be observed. These regions are of particular interest to us, as any potential civilization that would detect transiting planets around the Sun might have a reason to try and send us deliberate messages in trying to establish contact. This argument, in turn, could serve as a guide for our own search for extraterrestrial intelligence (SETI; Filippova & Strelnitskij 1988; Castellano, Doyle & McIntosh 2004; Conn Henry, Kilston & Shostak 2008; Nussinov 2009; Heller & Pudritz 2016).

2 METHODS

2.1 Definition of transit zones

A transit visibility zone – or simply transit zone – is the projection of a planet on to the celestial plane, from where it is possible to

★ E-mail: rwells02@qub.ac.uk
[1] http://exoplanet.eu (Schneider et al. 2011)
[2] http://phl.upr.edu/projects/habitable-exoplanets-catalog (Planetary Habitability Laboratory, University of Puerto Rico at Arecibo).

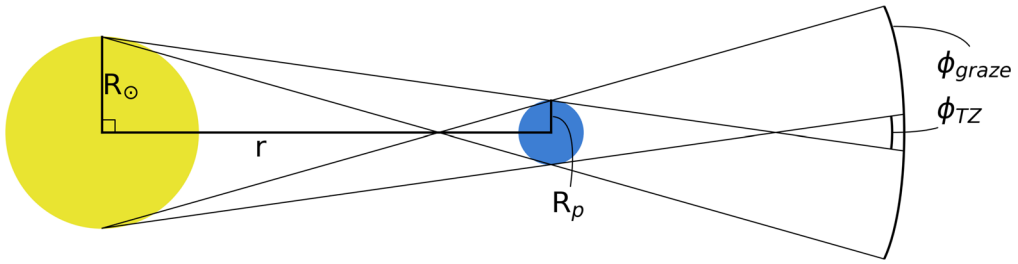

Figure 1. The transit zone of a planet (centre) projected out from the Sun (left-hand side). Sizes and distance not to scale.

detect transits of the planet in front of the Sun. Fig. 1 shows the geometry and construction of a Solar system planet's transit zone. Using trigonometry, $\phi_{\rm TZ}$, the angle in which an observer would see a full transit and $\phi_{\rm graze}$, the angle to observe a grazing transit, are given by (Heller & Pudritz 2016)

$$\phi_{\rm TZ} = 2\left(\arctan\left(\frac{\rm R_\odot}{r}\right) - \arcsin\left(\frac{R_{\rm p}}{\sqrt{(r^2+{\rm R}_\odot^2)}}\right)\right), \quad (1)$$

$$\phi_{\rm graze} = 2\arctan\left(\frac{(R_{\rm p}+{\rm R}_\odot)}{r}\right), \quad (2)$$

where $\rm R_\odot$ is the radius of the Sun, $R_{\rm p}$ is the radius of the planet and r is the instantaneous distance between the Sun and the planet, which varies over the course of the planet's orbit if it has non-zero eccentricity. This distance can be written as $r = a(1-e^2)/(1+e\cos(\theta))$ where a is the semimajor axis, e is the eccentricity and θ is the true anomaly – the angle between the planet's current position and the point in the orbit when it is closest to the Sun.

We note that $\phi_{\rm TZ}$ is commonly approximated by $2R_\star/a$ (Borucki & Summers 1984). As we show below, this works well for small planets at large separations. However, geometric transit probabilities obtained for larger Solar system planets differ to the results obtained via equation (1) by up to 21 per cent (see Section 3.3). We note that this approximation is widely used in the community even when it does not hold, in particular for exoplanets that have a small semimajor axis, including those orbiting late-M dwarfs and hot Jupiters. For example, TRAPPIST-1g (Gillon et al. 2017), a temperate Earth-sized planet orbiting an M8 star, gives a 10 per cent difference between equation (1) and the approximation, which is close to the largest disagreement in the Solar system (Jupiter, 11 per cent). This therefore has an impact on the statistics of exoplanetary systems, such as the occurrence rate, which is computed with the approximation (e.g. Howard et al. 2012; Dressing & Charbonneau 2015).

2.2 Numerical determination of transit zones

In order to calculate the transit zone angles, we collected values of the planetary radii, semimajor axes and the radius of the Sun from the NASA planetary fact sheets,[3] which are compiled from recent literature. For the planetary radii, the volumetric mean value was used; i.e. the radius of a sphere with the same volume as the body.

The transit zone and grazing angles ($\phi_{\rm TZ}$ and $\phi_{\rm graze}$ in Fig. 1) for the Solar system planets are given in Table 1 computed using equations (1) and (2). We also list the expected transit depths $\Delta F = (R_{\rm p}/{\rm R}_\odot)^2$. The relative differences between the angles of the full and grazing transit zones, calculated as per $\Delta\phi = \phi_{\rm graze}/\phi_{\rm TZ} - 1$, are also given. Variations are largest for large planets with small transit zones, such as Jupiter and Saturn. These differences are discussed more in detail in Section 3. Table 1 also serves as a comparison of how detectable each planet is, where a larger $\phi_{\rm TZ}$ suggests more possible extrasolar observers of the respective planetary transits and ΔF implies easier detection of the transit feature.

Table 1. The transit zone angles and transit depths of the Solar system planets.

Planet	$\phi_{\rm TZ}$ (°)	$\phi_{\rm graze}$ (°)	$\Delta\phi$ (%)	ΔF (%)
Mercury	1.3714	1.3810	0.7	0.0012
Venus	0.7301	0.7429	1.8	0.0076
Earth	0.5279	0.5376	1.8	0.0084
Mars	0.3479	0.3513	1.0	0.0024
Jupiter	0.0921	0.1127	22.4	1.0104
Saturn	0.0512	0.0605	18.3	0.7010
Uranus	0.0268	0.0288	7.6	0.1330
Neptune	0.0171	0.0183	7.3	0.1253

To calculate the positions of the transit zones on the celestial plane, we obtained orbital data from JPL HORIZONS,[4] where a single complete orbit of each planet was taken in the heliocentric ecliptic coordinate system. In heliocentric ecliptic coordinates, Earth's transit zone is a roughly 0.°53 wide disc of constant latitude at ecliptic latitude $b = 0$ (see Heller & Pudritz 2016). The other Solar system planets describe sinusoidal tracks determined by their Keplerian orbital elements. In order to make identifications of overlapping transit visibility zones more convenient, those discrete numerical values were fitted with functions of the form

$$l = A\sin(b - d), \quad (3)$$

where l is the longitude and b is the latitude. A is the planet's orbital inclination with respect to the ecliptic and d is related to the planet's argument of the periastron. We treated both A and d as are free parameters in our fitting procedure. The upper and lower bounds of the transit visibility zones were then created by adding and subtracting the value of $(\phi_{\rm TZ}/2)$ at each point along the orbit, respectively. This is a slight approximation; the exact transit zone borders would be derived by converting into planet-ecliptic coordinates before adding/subtracting the angle. Therefore by neglecting this step, the thickness of the transit zones are marginally thinner towards $b = 0$. We computed the minimum (at $b = 0$) and maximum (at maximum latitude $l_{\rm peak}$ of a given planet in ecliptic coordinates) distances between the upper and lower boundaries and then by comparing the difference between these distances, we estimated the change in thickness of the zones. Due to the small angles

[3] http://nssdc.gsfc.nasa.gov/planetary/planetfact.html (Curator: D.R. Williams, NSSDCA).

[4] http://ssd.jpl.nasa.gov/horizons.cgi (Giorgini et al. 1996).

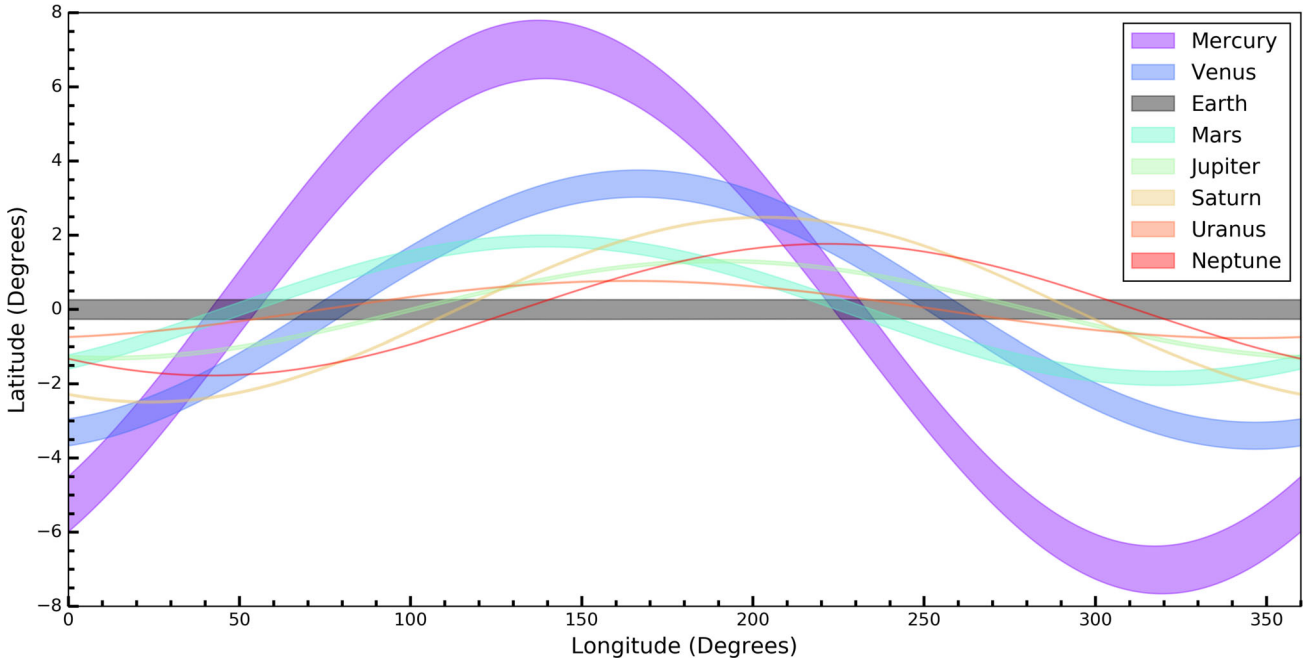

Figure 2. Projections of the transit visibility zones (non-grazing) of all the Solar system planets in heliocentric ecliptic coordinates. Each planet's transit zone is defined as a coloured bounded region.

involved, we find this is at most an effect of 0.7 per cent in thickness for Mercury, less than 0.2 per cent for the other planets and no effect for Earth as the ecliptic coordinate system is coplanar with Earth's orbit. We therefore decided to work with the approximated transit visibility zones.

The transit zones were computed using only one orbit of data, which we have assumed to be stationary. However, the shapes and positions of the transit zones would change slightly over the course of many orbits due to orbital precession from planet–planet interactions, the motion of the Sun from interacting with Jupiter and any planet–moon interactions (Heller & Pudritz 2016). We calculated how long the transit zones would be valid by taking values[5] for the change in longitude of perihelion from Standish & Williams (1992) (roughly 0.°3 per century, excluding Venus) which we assume to be constant and comparing them to half the width of the transit zones. From this we found that the transit zones of the terrestrial planets would be valid for thousands of years, while the smaller transit zones of the Jovian planets would be valid for hundreds of years. However, Venus precesses two orders of magnitude slower than the other planets and therefore its transit zone would be valid for a few hundred thousand years. We also note that stars are not fixed in the sky and instead have proper motions of around 1 arcsec yr^{-1} for nearby stars ($<$10 pc) and around 100 mas yr^{-1} for more distant stars ($>$20 pc). This means that nearby and more distant stars centred in the transit zone of Earth would leave the zone after roughly 1 000 and 10 000 yr, respectively, if they were moving perpendicular to the boundaries. These time-scales are 3 times longer for traversing the transit zone of Mercury and 30 times shorter for the case of Neptune, simply by comparing the relative sizes of $\phi_{\rm TZ}$.

Time-scales for the overlap regions of transit zones are more complex due to their various sizes and the movement of multiple transit zones. We give one example here, for Mars–Jupiter, which consists of two areas with width of $\sim$14°. We took the central point of one of the areas and then precessed the transit zones through time until the central point at $t = 0$ was no longer inside the overlap region. We found that the transits of Mars and Jupiter would both be observable for approximately 1700 yr. We also find that nearby and more distant stars would cross the nearest overlap region border in 140 and 1400 yr, respectively, if moving perpendicular to the border. Other overlapping regions will be observable for different amounts of time due to their various sizes and mutual precession speeds. The code to produce the tables and figures in this work is available on GitHub.[6]

3 RESULTS

3.1 Location of transit zones in the sky

We show the locations of the transit zones of the Solar system planets in Fig. 2. All sets of the planets' transit zones were searched for mutual overlaps from where multiple planets could be detected. Observers here would see our Solar system similarly to how we see transiting multiplanet systems. It can be seen from Fig. 2 that the maximum number of different transits visible from any one point in the sky is three. This shows that exoplanetary systems with multiple transiting planets may still hide further companions, as highlighted by Kane & Gelino (2013). Different sets of three planets can be observed to transit from different points in the sky, which we find in agreement with Brakensiek & Ragozzine (2016).

Specifically, we find 28 two-planet and 8 three-planet sets, each of which comprises two overlapping regions in opposite directions on the celestial plane that are offset by roughly 180° of longitude, except for the Mercury–Earth–Uranus set. Fig. 3 shows a zoom into one region of Mars–Jupiter and one region of the Mercury–Earth–Mars overlapping regions to give an idea of the shapes and sizes of these areas. All sets of planets where overlap exist are given in

[5] https://ssd.jpl.nasa.gov/txt/p_elem_t1.txt

[6] https://github.com/ExoRob/Transit-Zones

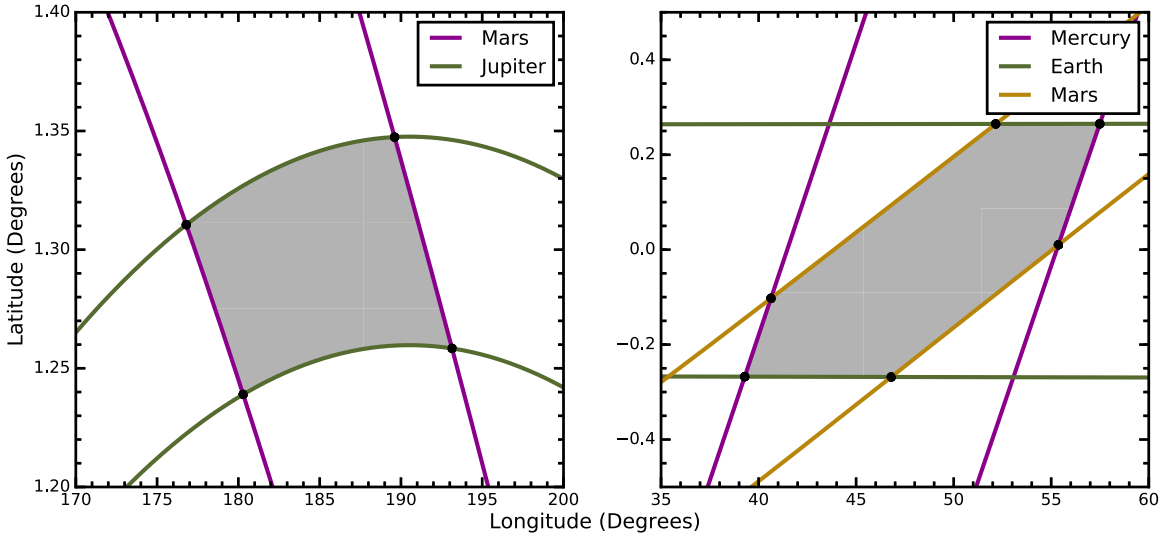

Figure 3. Examples of regions where the non-grazing transit zones intersect, given in ecliptic coordinates. The black circles are the points where the lines intersect – equatorial coordinates of these points are given in Appendix A for all overlap regions.

Appendix A with equatorial coordinates of the intersection points, converted using the SKYCOORD ASTROPY PYTHON package (Astropy Collaboration et al. 2013) with a distance of 30 ly. A distance is required due to the origin shift when converting between heliocentric and geocentric coordinate systems. A distance of 30 ly was chosen because stars of interest are typically farther away than ca. 10 pc, and assuming greater distances did not change computed coordinates past 10^{-5} degrees (0.04 arcsec). The coordinates are provided to be used as a quick check as to whether any given star falls into a transit zone.

3.2 Probabilities to observe Solar system planet transits

By comparing the solid angle covered by each transit zone to the area of the whole sky (4π), it is possible to obtain the probabilities of each planet to be transiting for a randomly positioned extrasolar observer. The probabilities of each overlap region were also found in the same manner, and are given in Appendix B, both as the absolute probability and as a factor of the probability to detect Earth. For individual planets, the area of the transit zones were calculated by using the trapezoidal rule to find the area beneath each of the boundaries. Subtracting the area below the lower boundary from the upper boundary gave the area of the transit zone. For the two- and three-planet overlap region cases, first the curves defining the boundaries of each region were found. Then the areas were found the same way as in the single planet case. Adding these areas together then gave the total area for the set of planets. The areas for all cases were then converted into steradians, and divided by 4π to return geometric transit probabilities.

The probabilities of a randomly positioned extrasolar observer being able to observe at least one, two, or three transits were calculated by adding up the individual transit probabilities listed in Table B, giving

(i) $P_1 = 2.518$ per cent to observe at least one transiting planet;
(ii) $P_2 = 0.229$ per cent to observe at least two transiting planets; and
(iii) $P_3 = 0.027$ per cent to observe three transiting planets.

These probabilities were calculated simply from Table B1 and are therefore only applicable to observing the Solar system.

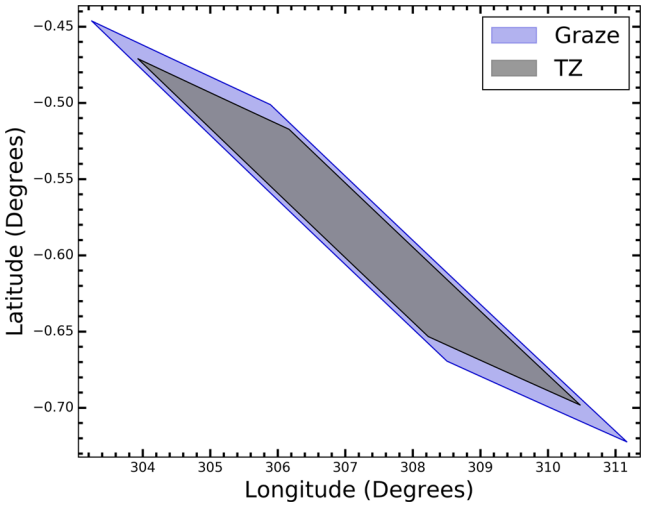

Figure 4. Comparison of the regions where grazing transits (blue) and full transits (grey) of both Jupiter and Saturn could be observed, given in heliocentric ecliptic coordinates. The area of the blue region is approximately 45 per cent larger than the area of the grey region.

Exoplanetary systems will have different coplanarity and multiplicity that will consequently lead to different probabilities. Using the values given in Table B, we then calculate the probability of an observer inside the Earth's transit zone to be able to see other Solar system planets in transit as well. We find that an observer viewing transits of Earth would have a 24 per cent chance of detecting at least one more planet in the Solar system via transits, purely from a geometric point of view.

The regions where an extrasolar observer could detect grazing transits of multiple planets are significantly larger for some sets. This is simply due to the grazing angle being larger than the transit zone angle (see Table 1), in particular for cases involving the gas giants. This effect is also more apparent for the Jovian planets because their transit zones are smaller due to their semimajor axes being much larger than those of the terrestrial planets. For example, the grazing region between Jupiter and Saturn can be seen in Fig. 4, which is 45 per cent larger compared to the full transit zone of these

Table 2. Comparison of probabilities computed using ϕ_{TZ} and the approximation, 2R/a. A full table of results using ϕ_{TZ} is given in Appendix B.

Set of planets	P(ϕ_{TZ})	P($2R/a$)	ΔP (%)
Mercury, Mars	2.73×10^{-4}	2.75×10^{-4}	− 0.9
Venus, Earth	3.16×10^{-4}	3.22×10^{-4}	− 1.8
Earth, Mars	2.80×10^{-4}	2.84×10^{-4}	− 1.4
Earth, Jupiter	1.05×10^{-4}	1.17×10^{-4}	− 12.2
Jupiter, Saturn	1.05×10^{-5}	1.27×10^{-5}	− 21.3
Uranus, Neptune	8.44×10^{-7}	9.08×10^{-7}	− 7.6
Mercury, Venus, Saturn	3.21×10^{-5}	3.52×10^{-5}	− 9.5
Mercury, Venus, Neptune	1.60×10^{-6}	1.74×10^{-6}	− 8.4
Mercury, Earth, Mars	2.08×10^{-4}	2.10×10^{-4}	− 1.2
Mercury, Earth, Uranus	3.89×10^{-8}	8.78×10^{-8}	− 125.6
Mercury, Mars, Uranus	4.62×10^{-6}	4.88×10^{-6}	− 5.7
Venus, Earth, Uranus	2.08×10^{-5}	2.18×10^{-5}	− 4.7
Mars, Jupiter, Neptune	2.19×10^{-6}	2.55×10^{-6}	− 16.8
Jupiter, Saturn, Uranus	1.96×10^{-6}	2.22×10^{-6}	− 13.3

two planets. Therefore, searches can be extended by the inclusion of regions where grazing transits can be detected and would give significantly more area of the sky for sets that include Jovian planets.

3.3 Differences to approximate calculations

Table 2 shows a comparison of probabilities computed using the transit zone angle to those calculated using an estimate of $2\,R_\odot/a$, an approximation originally proposed by Borucki & Summers (1984). The values we obtain for the terrestrial planet overlap regions match well with the approximation, whereas the Jovian planet overlap regions differ by up to 21 per cent. The Mercury–Earth–Uranus region shows an extremely large discrepancy between the approximation and the exact calculation; this is due to the region's small size, where small changes in the transit zone thickness change the area by relatively large amounts. The discrepancies for the other sets of planets are due to the approximation treating planets as point objects, i.e. ignoring the planetary radius. Therefore, the approximation significantly overestimates transit probabilities for overlap regions that include the giant planets, as seen in Table 2.

4 DISCUSSION

4.1 Exoplanets within the Solar system transit zones

All known exoplanets situated within a transit zone of a Solar system planet are given in Appendix C. This list is up-to-date as of March 2017 with information from exoplanet.eu, and contains 65 confirmed and 3 unconfirmed planets. The list is slightly disproportionate due to the inclusion of 43 exoplanets that only fall into Mercury's transit zone. We note, however, that 9 planets have already been found in the Earth's transit zone, though none are expected to be habitable due to their size and stellar radiation received. Of particular interest is EPIC211913977 b (K2-101b, Mann et al. 2017) – a planet on the border between super-Earth and mini-Neptune from whose position transits of Jupiter, Saturn and Uranus can be detected. In addition, a hot-Jupiter falls into the transit zones of both Earth and Jupiter and a further three planets fall into the overlap region between Venus and Mars.

The Kepler space telescope will help improve the detection statistics of exoplanets that fall into transit zones. After the second of four reaction wheels failed on the *Kepler* spacecraft on 2013 May 11, the telescope was re-purposed into the ongoing *K2* mission (Howell et al. 2014). *K2* observations entail a series of observing 'campaigns' of fields that are limited by Sun angle constraints to a duration of approximately 80 d each. Although *K2* therefore focuses on detecting short-period exoplanets, this does not rule out finding targets of interest for SETI. Planets in tight orbits have been found in the HZ around M-dwarfs, such as planets e, f and g in the TRAPPIST-1 system, which have periods of 6.06, 9.1 and 12.35 d, respectively (Gillon et al. 2017). The spacecraft is now kept steady by the radiation pressure from the Sun, which means that the telescope must be aligned with the ecliptic and therefore gives a large amount of targets residing in the transit visibility zones of the Solar system planets. Approximately 4000 targets are observed per campaign in these regions, which corresponds to around 12 transiting exoplanet candidates per campaign assuming the value of 3×10^{-3} candidates per target from Pope, Parviainen & Aigrain (2016). Fig. 5 shows all past and finalized future *K2* fields at the date of publishing, overplotted with the transit zones of the Solar system planets from Fig. 2.

4.2 Earth analogues in transit zones

Currently no terrestrial exoplanets in HZs around their host stars are known to be located in any of the Solar system planet transit zones. Nevertheless, we can estimate how likely such planets are to occur within a certain volume.

There are 1022 known G and K dwarf stars listed in the SIMBAD data base (Wenger et al. 2000) that reside in Earth's transit zone with a *V* magnitude of less than 13, which is the limiting brightness for terrestrial planets in the *PLATO* mission (Rauer et al. 2014). It is possible to estimate the number of temperate rocky planets around these stars by approximating the frequency of Earth-size planets within the HZ of Sun-like stars ($\eta_\oplus$). Batalha (2014) evaluated $\eta_\oplus$ to be 22 ± 8 per cent for a radius range of 0.5–1.4$R_\oplus$ around G and K stars using the results of Petigura et al. (2013), which corresponds to roughly 225 ± 82 Earth analogues in this sample of GK stars in Earth's transit zone.

By combining this with the probability of Earth transiting for a randomly position observer (0.46 per cent from Table B1), this gives a statistical estimate of 1.0 ± 0.4 transiting planets around the known Sun-like stars that resides in Earth's transit visibility zone. The estimate is small due to the low number of known stars out to 13 mag; i.e. the incompleteness of the catalogue. By comparing the number of known GK stars at set magnitudes to the volume increase, we estimated the true number of GK stars with $V < 13$ in the Earth's transit zone to be roughly 3150. Using this value instead gives 3.2 ± 1.2 transiting temperate Earth-sized planets, where the uncertainty comes from the uncertainty in the value of $\eta_\oplus$. We note that this is a rather optimistic estimate, due to using boundaries of the 'simple' HZ (incident stellar energy 0.25–4$F_\oplus$). To date, Kepler-452b (Jenkins et al. 2015) remains the only exoplanet discovered that comes close to meeting these temperate and Earth-sized requirements; it is a 1.6$R_\oplus$ planet which orbits a 13.7 V magnitude G2 star of mass of 1.0 $M_\odot$ at a distance of 1.05 au. However, it does not fall into any Solar system planet transit zone and is unlikely to be rocky (Rogers 2015; Chen & Kipping 2017).

We also estimated the expected number of temperate Earth-sized planets orbiting M-dwarfs in the Earth's transit zone using the same method used for GK stars. To do this we took a system of an M3 star with an Earth-sized planet orbiting in the centre of the HZ. From this we find the probability that a planet will transit to be 1.44 per cent, using values for an M3 star from Kaltenegger & Traub (2009). We take the limiting *V* magnitude for a detection to

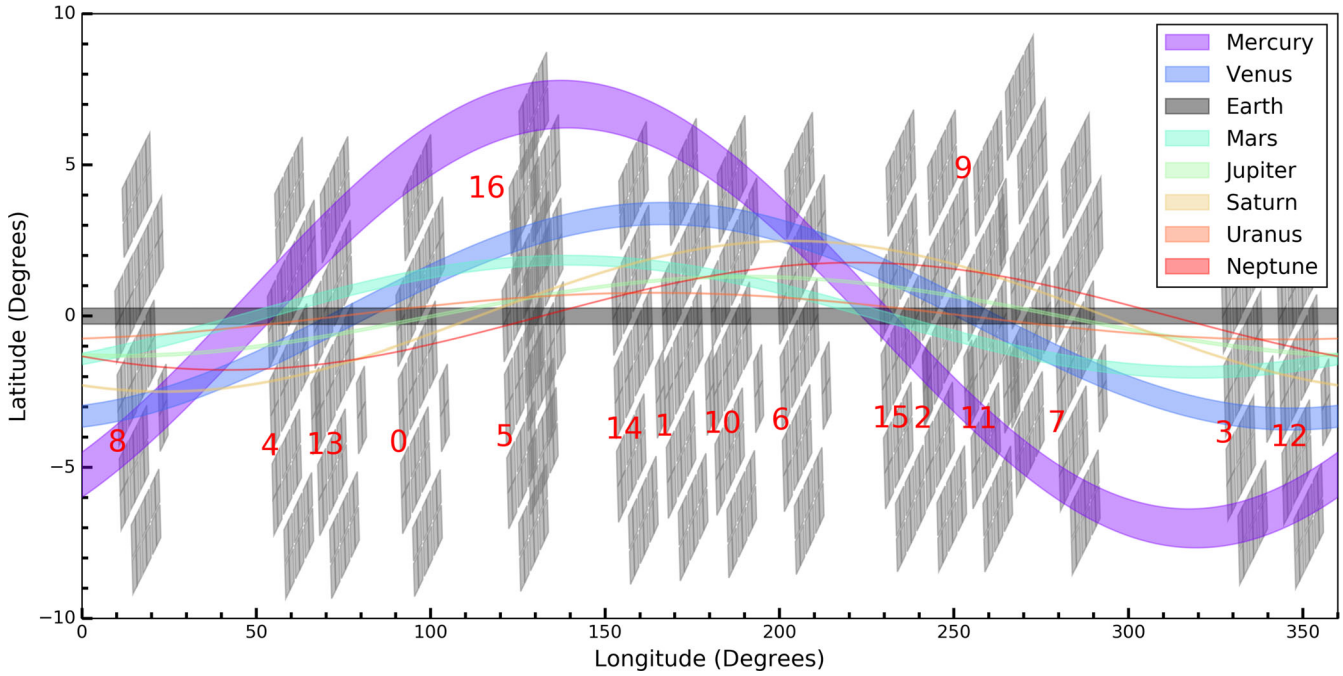

Figure 5. As Fig. 2, with the fields of the *K2* mission overlaid. The campaign number is given in red for each field.

be 16 mag, which gives approximately 673 M-dwarfs in the Earth's transit zone after accounting for completeness as before. We use the occurrence rate of $0.68^{+0.13}_{-0.08}$ Earth-sized (0.5–1.4$R_\oplus$) planets per M-dwarf from Dressing & Charbonneau (2015), which again are in the 'simple' HZ for comparison. This gives an expected $6.6^{+1.3}_{-0.8}$ Earth-sized planets in the HZ around M-dwarf hosts brighter than 16 mag, which reside in the Earth's transit zone.

Transit visibility zones of the Solar system planets are particular areas of interest for programs that search for extraterrestrial intelligent life, such as the SETI program (see Tarter 2001, and references therein) that has recently gained momentum by the Breakthrough Listen Initiative (Isaacson et al. 2017). Intelligent observers in these transit visibility zones could identify Earth as a habitable world and attempt communication, possibly via beamed radio transmissions. Defining regions of the sky where artificial signals are potentially more likely can cut down the area of the sky required for SETI-type programs to only 0.46 per cent of the complete sky. Assuming the same sensitivity as the Kepler space telescope, transits of Earth could be detected out to roughly 275 pc, assuming a signal-to-noise ratio > 8 and more than three transits – i.e. 3 yr or more of continuous data. However, with better technology or data spanning a longer time frame, transits of Earth could be observed out to the edges of the HZ of the Galaxy ($\sim$1 kpc from Earth, Lineweaver, Fenner & Gibson 2004). In addition to the references in the introduction, transits of Earth and exoplanets have been discussed in the context of extraterrestrial intelligence (Kipping & Teachey 2016; Forgan 2017).

5 CONCLUSIONS

We identified the regions of the sky where an observer could detect transits of one or more Solar system planets. The coordinates of these regions have been supplied in Appendix A. The probabilities of detecting transits of a single Solar system planet, as well as set of planets with overlapping transit visibility zones, are given in Appendix B. These probabilities have been calculated using the exact equation for the transit angles, which is more precise than those derived using the commonly known approximation of $2\,R_\odot/a$. It is not possible to observe transits of more than three Solar system planets from any extrasolar perspective. Detecting two or three Solar system planets via transits is possible, but rather unlikely (see Appendix B). We find a 24 per cent chance for an extrasolar observer with the favourable geometry to see the Earth's solar transit to also observe at least one more Solar system planet in transit.

Sixty-eight of the currently known exoplanets or candidates fall into the transit zones of the Solar system planets Appendix C. The list includes nine planets in Earth's transit zone, one planet in a triple-overlap region and four planets in a double-overlap region. None of these planets, however, are expected to harbour life due to their various physical parameters such as mass and radiation received.

The ongoing *K2* mission will detect many exoplanets within the transit zones of the Solar system planets – we expect *K2* to discover approximately 12 exoplanet candidates per campaign in these zones. Although all planets found will be relatively fast-orbiting, this does not rule out habitable planets that orbit around M-dwarf stars.

We derived a statistical estimate of three temperate Earth-sized planets in orbits around Sun-like stars that fall in Earth's transit zone, one of which may be detected by the upcoming *PLATO* mission. Looking at these systems would be similar to seeing the Earth from outside the Solar system, and would be high priority targets for searches for biomarkers and even extraterrestrial intelligence due to the possibility of life and the mutual detection of each other's transits.

ACKNOWLEDGEMENTS

RW thanks the Northern Ireland Department for Education for the award of a PhD studentship. CAW acknowledges support from STFC grant ST/P000312/1. This work was supported in part by the German space agency (Deutsches Zentrum für Luft- und Raumfahrt) under PLATO Data Center grant 50OO1501.

REFERENCES

Anglada-Escudé G. et al., 2013, A&A, 556, A126
Anglada-Escudé G. et al., 2016, Nature, 536, 437
Astropy Collaboration et al., 2013, A&A, 558, A33
Barnes R., Heller R., 2013, Astrobiology, 13, 279
Batalha N. M., 2014, Proc. Natl. Acad. Sci., 111, 12647
Borucki W. J., Summers A. L., 1984, Icarus, 58, 121
Brakensiek J., Ragozzine D., 2016, ApJ, 821, 47
Castellano T., Doyle L., McIntosh D., 2004, in Penny A., ed., Proc. IAU Symposium 202, Planetary Systems in the Universe. Kluwer, Dordrecht, p. 445
Chen J., Kipping D., 2017, ApJ, 834, 17
Conn Henry R., Kilston S., Shostak S., 2008, in American Astronomical Society Meeting Abstracts #212. p. 194
Dressing C. D., Charbonneau D., 2015, ApJ, 807, 45
Filippova L. N., Strelnitskij V. S., 1988, Astronomicheskij Tsirkulyar, 1531, 31
Forgan D. H., 2017, preprint (arXiv:1707.03730)
Gillon M. et al., 2017, Nature, 542, 456
Giorgini J. D. et al., 1996, in AAS/Division for Planetary Sciences Meeting Abstracts #28. p. 1158
Heller R., Pudritz R. E., 2016, Astrobiology, 16, 259
Howard A. W. et al., 2012, ApJS, 201, 15
Howell S. B. et al., 2014, PASP, 126, 398
Isaacson H. et al., 2017, PASP, 129, 054501
Jenkins J. M. et al., 2015, AJ, 150, 56
Kaltenegger L., Traub W. A., 2009, ApJ, 698, 519
Kane S. R., Gelino D. M., 2013, ApJ, 762, 129
Kasting J. F., Whitmire D. P., Reynolds R. T., 1993, Icarus, 101, 108
Kipping D. M., Teachey A., 2016, MNRAS, 459, 1233
Kopparapu R. K. et al., 2013, ApJ, 765, 131
Lineweaver C. H., Fenner Y., Gibson B. K., 2004, Science, 303, 59
Mann A. W. et al., 2017, AJ, 153, 64
Nussinov S., 2009, preprint (arXiv:0903.1628)
Pepe F. et al., 2013, Nature, 503, 377
Petigura E. A., Howard A. W., Marcy G. W., 2013, Proc. Natl. Acad. Sci., 110, 19273
Pope B. J. S., Parviainen H., Aigrain S., 2016, MNRAS, 461, 3399
Rauer H. et al., 2014, Exp. Astron., 38, 249
Reynolds R. T., McKay C. P., Kasting J. F., 1987, Adv. Space Res., 7, 125
Rogers L. A., 2015, ApJ, 801, 41
Schneider J., Dedieu C., Le Sidaner P., Savalle R., Zolotukhin I., 2011, A&A, 532, A79
Standish E. M., Williams J. G., 1992, Orbital ephemerides of the Sun, Moon, and planets. University Science Books Mill Valley, CA
Tarter J., 2001, ARA&A, 39, 511
Vogt S. S., Butler R. P., Rivera E. J., Haghighipour N., Henry G. W., Williamson M. H., 2010, ApJ, 723, 954
Wenger M. et al., 2000, A&AS, 143, 9

APPENDIX A: OVERLAP REGIONS OF TRANSIT VISIBILITY ZONES OF SOLAR SYSTEM PLANETS

Table A1. Overlap regions of all the Solar system planets, given in equatorial coordinates. Each set has two overlap regions, separated by roughly 180°, with the exception of the Mercury, Earth and Uranus overlap region. Coordinates are given for both individual overlap regions, with each region's coordinates on a separate row.

Planets	RA (°)	Dec. (°)
Mercury, Venus	11.7015, 20.1091, 31.2765, 40.6216	1.2788, 5.8413, 9.7849, 14.1528
	193.1873, 202.1523, 208.7497, 217.5191	−1.9486, −6.7372, −8.7483, −13.0101
Mercury, Earth	36.9870, 41.0814, 50.7379, 55.1542	14.3382, 16.1807, 18.2795, 19.8598
	218.9127, 223.0575, 228.5762, 232.7704	−14.9577, −16.7615, −17.7374, −19.3130
Mercury, Mars	34.4691, 38.2540, 53.0315, 57.1011	13.1559, 14.9191, 19.1176, 20.5116
	217.0902, 220.7140, 230.0600, 233.8370	−14.1317, −15.7547, −18.3091, −19.6934
Mercury, Jupiter	29.3177, 30.1135, 43.9977, 44.8553	10.6326, 11.0310, 15.6051, 15.9623
	211.1509, 211.9035, 221.7918, 222.5512	−11.3130, −11.6802, −14.9305, −15.2600
Mercury, Saturn	19.6025, 20.0142, 33.3310, 33.7779	5.5699, 5.7906, 10.7851, 10.9999
	200.9720, 201.3855, 211.5137, 211.9181	−6.1163, −6.3342, −10.1334, −10.3331
Mercury, Uranus	35.4333, 35.6512, 50.5541, 50.7928	13.6128, 13.7154, 18.2107, 18.3000
	217.4555, 217.6955, 228.1101, 228.3516	−14.2989, −14.4083, −17.5547, −17.6495
Mercury, Neptune	25.8266, 25.9521, 38.7173, 38.8517	8.8527, 8.9175, 13.3024, 13.3632
	207.3073, 207.4350, 216.8692, 216.9966	−9.3973, −9.4620, −12.7084, −12.7677
Venus, Earth	63.9972, 73.6155, 77.2616, 87.1343	21.0167, 22.8535, 22.6528, 23.6808
	244.1603, 253.5242, 257.3530, 266.9091	−21.0507, −22.8362, −22.6683, −23.6680
Venus, Mars	110.0730, 120.6906, 85.9473, 97.0947	23.5889, 22.3728, 24.3262, 24.7999
	265.6867, 277.7724, 289.2227, 301.3848	−24.3019, −24.7984, −23.6588, −22.2724
Venus, Jupiter	50.5135, 52.9740, 69.8012, 72.3726	17.4529, 18.1865, 21.4512, 21.9065
	230.6284, 232.9169, 249.8003, 252.2384	−17.4869, −18.1687, −21.4535, −21.8865
Venus, Saturn	18.4418, 19.7970, 37.7801, 39.2221	5.1046, 5.7040, 12.3267, 12.8635
	198.4127, 199.7273, 217.8311, 219.1757	−5.0937, −5.6752, −12.3456, −12.8464
Venus, Uranus	67.4052, 68.0222, 84.6971, 85.3428	21.7360, 21.8582, 23.4867, 23.5419
	247.4526, 248.0827, 264.6176, 265.2576	−21.7431, −21.8677, −23.4831, −23.5382
Venus, Neptune	35.8160, 36.1561, 50.6768, 51.0326	12.3626, 12.4928, 16.7364, 16.8447
	215.8121, 216.1470, 230.6600, 231.0091	−12.3614, −12.4897, −16.7322, −16.8386
Earth, Mars	33.1817, 44.4152, 49.6725, 61.2482	13.0659, 16.6004, 18.5652, 21.0835
	213.7997, 224.2269, 229.7480, 240.9652	−13.2811, −16.5519, −18.5785, −21.0248

Table A1 *– continued*

Planets	RA (°)	Dec. (°)
Earth, Jupiter	111.9535, 116.3318, 86.1188, 90.6865	22.1766, 21.5066, 23.1223, 23.1688
	266.6015, 271.0545, 291.5136, 295.9531	−23.1419, −23.1753, −22.2285, −21.5605
Earth, Saturn	108.0923, 109.4330, 121.3168, 122.6180	22.1264, 21.9660, 20.5977, 20.3351
	288.3799, 289.5843, 301.1709, 302.3523	−22.1018, −21.9561, −20.6178, −20.3809
Earth, Uranus	50.2518, 52.3607, 93.4203, 95.7638	18.1588, 18.6723, 23.6698, 23.6014
	230.6594, 232.8785, 272.6986, 274.9796	−18.2660, −18.8004, −23.6751, −23.6195
Earth, Neptune	124.9518, 125.5307, 142.6482, 143.1965	19.2871, 19.1582, 15.0190, 14.8417
	305.2351, 305.8100, 322.4193, 322.9703	−19.2328, −19.1038, −15.0851, −14.9077
Mars, Jupiter	10.2013, 13.7149, 356.2880, 359.8240	2.9218, 4.5116, −3.0317, −1.4173
	177.5839, 180.7676, 189.3645, 192.5865	2.4753, 1.0176, −2.5706, −4.0320
Mars, Saturn	156.3063, 157.5163, 163.6807, 164.8623	11.6364, 11.1583, 8.9726, 8.4712
	335.5695, 336.7211, 344.4525, 345.5888	−11.8888, −11.4378, −8.6811, −8.1960
Mars, Uranus	22.7045, 23.8867, 39.7803, 41.0040	8.8540, 9.3518, 15.0634, 15.4810
	203.6493, 204.9001, 219.0955, 220.4226	−9.2290, −9.7519, −14.8405, −15.2975
Mars, Neptune	357.9897, 358.3683, 6.4707, 6.8470	−2.2563, −2.0834, 1.2162, 1.3888
	178.6744, 179.0460, 185.8387, 186.2121	1.9770, 1.8069, −0.9576, −1.1288
Jupiter, Saturn	126.3296, 128.8754, 130.6375, 133.1409	19.7400, 19.1920, 18.8831, 18.2798
	306.3716, 308.6853, 310.8305, 313.1306	−19.7298, −19.2326, −18.8398, −18.2845
Jupiter, Uranus	127.4931, 129.8344, 135.0180, 137.3045	19.5875, 19.0687, 17.7098, 17.1015
	307.4337, 309.6116, 315.2746, 317.4065	−19.6019, −19.1212, −17.6409, −17.0713
Jupiter, Neptune	175.4018, 176.3556, 180.3649, 181.3143	3.3075, 2.9026, 1.2860, 0.8789
	0.6033, 1.5658, 355.1585, 356.1218	−1.1885, −0.7757, −3.4060, −2.9974
Saturn, Uranus	129.5076, 130.3481, 131.1154, 131.9524	19.1184, 18.9441, 18.7263, 18.5448
	309.6050, 310.3891, 311.0756, 311.8565	−19.0961, −18.9331, −18.7372, −18.5680
Saturn, Neptune	76.0659, 77.1420, 79.4563, 80.5380	21.3616, 21.4899, 21.6875, 21.7941
	256.2442, 257.3057, 259.2907, 260.3563	−21.3806, −21.5060, −21.6733, −21.7794
Uranus, Neptune	158.6035, 159.2136, 159.6183, 160.2270	9.7970, 9.5578, 9.4284, 9.1875
	338.6460, 339.2602, 339.5715, 340.1844	−9.7817, −9.5408, −9.4456, −9.2031
Mercury, Venus, Saturn	19.6025, 20.0142, 33.3310, 33.7779	5.5699, 5.7906, 10.7851, 10.9999
	200.9720, 201.3855, 211.5137, 211.9181	−6.1163, −6.3342, −10.1334, −10.3331
Mercury, Venus, Neptune	35.8160, 36.1561, 38.7173, 38.8517	12.3626, 12.4928, 13.3024, 13.3632
	215.8121, 216.1470, 216.8692, 216.9966	−12.3614, −12.4897, −12.7084, −12.7677
Mercury, Earth, Mars	36.9870, 38.2540, 44.4152, 49.6725, 53.0315, 55.1542	14.3382, 14.9191, 16.6004, 18.5652, 19.1176, 19.8598
	218.9127, 220.7140, 224.2269, 229.7480, 230.0600, 232.7704	−14.9577, −15.7547, −16.5519, −18.5785, −18.3091, −19.3130
Mercury, Earth, Uranus	50.2518, 50.7379, 50.7928	18.1588, 18.2795, 18.3000
Mercury, Mars, Uranus	35.4333, 35.6512, 39.7803, 41.0040	13.6128, 13.7154, 15.0634, 15.4810
	217.4555, 217.6955, 219.0955, 220.4226	−14.2989, −14.4083, −14.8405, −15.2975
Venus, Earth, Uranus	67.4052, 68.0222, 84.6971, 85.3428	21.7360, 21.8582, 23.4867, 23.5419
	247.4526, 248.0827, 264.6176, 265.2576	−21.7431, −21.8677, −23.4831, −23.5382
Mars, Jupiter, Neptune	178.6744, 179.0460, 180.3649, 181.3143	1.9770, 1.8069, 1.2860, 0.8789
	0.6033, 1.5658, 357.9897, 358.3683	−1.1885, −0.7757, −2.2563, −2.0834
Jupiter, Saturn, Uranus	129.5076, 130.3481, 131.1154, 131.9524	19.1184, 18.9441, 18.7263, 18.5448
	309.6050, 310.3891, 311.0756, 311.8565	−19.0961, −18.9331, −18.7372, −18.5680

APPENDIX B: TRANSIT PROBABILITIES

Table B1. All non-zero transit probabilities of combinations of the Solar system planets, given as $1/N$ and $P/P_{\oplus}$.

Planets	Probability	Ratio to $P_{\oplus}$
Mercury	1.2×10^{-2}	2.7
Venus	6.4×10^{-3}	1.4
Earth	4.6×10^{-3}	1.0
Mars	3.1×10^{-3}	6.6×10^{-1}
Jupiter	8.1×10^{-4}	1.7×10^{-1}
Saturn	4.5×10^{-4}	9.7×10^{-2}
Uranus	2.3×10^{-4}	5.1×10^{-2}
Neptune	1.5×10^{-4}	3.2×10^{-2}
Mercury, Venus	6.7×10^{-4}	1.5×10^{-1}
Mercury, Earth	3.0×10^{-4}	6.5×10^{-2}
Mercury, Mars	2.7×10^{-4}	5.9×10^{-2}
Mercury, Jupiter	5.9×10^{-5}	1.3×10^{-2}
Mercury, Saturn	3.2×10^{-5}	7.0×10^{-3}
Mercury, Uranus	1.7×10^{-5}	3.6×10^{-3}
Mercury, Neptune	9.7×10^{-6}	2.1×10^{-3}
Venus, Earth	3.2×10^{-4}	6.9×10^{-2}
Venus, Mars	3.7×10^{-4}	8.0×10^{-2}
Venus, Jupiter	8.3×10^{-5}	1.8×10^{-2}
Venus, Saturn	5.1×10^{-5}	1.1×10^{-2}
Venus, Uranus	2.1×10^{-5}	4.5×10^{-3}
Venus, Neptune	1.2×10^{-5}	2.7×10^{-3}
Earth, Mars	2.8×10^{-4}	6.1×10^{-2}
Earth, Jupiter	1.0×10^{-4}	2.3×10^{-2}
Earth, Saturn	3.0×10^{-5}	6.6×10^{-3}
Earth, Uranus	5.2×10^{-5}	1.1×10^{-2}
Earth, Neptune	1.4×10^{-5}	3.1×10^{-3}
Mars, Jupiter	6.3×10^{-5}	1.4×10^{-2}
Mars, Saturn	2.1×10^{-5}	4.6×10^{-3}
Mars, Uranus	2.2×10^{-5}	4.8×10^{-3}
Mars, Neptune	7.0×10^{-6}	1.5×10^{-3}
Jupiter, Saturn	1.0×10^{-5}	2.3×10^{-3}
Jupiter, Uranus	9.8×10^{-6}	2.1×10^{-3}
Jupiter, Neptune	4.7×10^{-6}	1.0×10^{-3}
Saturn, Uranus	2.0×10^{-6}	4.2×10^{-4}
Saturn, Neptune	2.5×10^{-6}	5.4×10^{-4}
Uranus, Neptune	8.4×10^{-7}	1.8×10^{-4}
Mercury, Venus, Saturn	3.2×10^{-5}	7.0×10^{-3}
Mercury, Venus, Neptune	1.6×10^{-6}	3.5×10^{-4}
Mercury, Earth, Mars	2.1×10^{-4}	4.5×10^{-2}
Mercury, Earth, Uranus	3.9×10^{-8}	8.4×10^{-6}
Mercury, Mars, Uranus	4.6×10^{-6}	1.0×10^{-3}
Venus, Earth, Uranus	2.1×10^{-5}	4.5×10^{-3}
Mars, Jupiter, Neptune	2.2×10^{-6}	4.7×10^{-4}
Jupiter, Saturn, Uranus	2.0×10^{-6}	4.2×10^{-4}

APPENDIX C: EXOPLANETS IN TRANSIT ZONES

Table C1. Sixty-eight confirmed and unconfirmed exoplanets that fall within one or more transit zones of the Solar system planets. Data from http://exoplanet.eu.

Planet identifier	Status	RA, Dec. (°)	In zones	Total
EPIC 211913977 b	Confirmed	130.3441, 18.9339	Jupiter, Saturn, Uranus	3
HATS-11 b	Confirmed	289.4000, −22.3900	Earth, Jupiter	2
HD 181342 b	Confirmed	290.2667, −23.6194	Venus, Mars	2
HD 50554 b	Confirmed	103.6750, 24.2456	Venus, Mars	2
K2-26 b	Confirmed	94.2083, 24.5958	Venus, Mars	2
11 Oph b	Confirmed	245.6042, −24.0872	Mercury	1
1RXS 1609 b	Confirmed	242.3750, −21.0828	Earth	1
2M 0441+23 b	Confirmed	70.4375, 23.0308	Mars	1
BD+20 594 b	Confirmed	53.6500, 20.5992	Mercury	1
EPIC 216468514 b	Confirmed	284.9854, −22.2934	Saturn	1
GJ 785 b,c	Confirmed	303.8208, −27.0331	Mercury	1
GJ 876 b,c,d,e	Confirmed	343.3042, −14.2536	Mercury	1
GJ 876 f,g	Unconfirmed	343.3042, −14.2536	Mercury	1
GSC 6214−210 b	Confirmed	245.4792, −20.7186	Venus	1
HAT-P-50 b	Confirmed	118.0625, 28.1394	Mercury	1
HATS-3 b	Confirmed	312.4583, −24.4289	Mercury	1
HD 164604 b	Confirmed	270.7792, −28.5606	Mercury	1
HD 171238 b	Confirmed	278.6833, −28.0722	Mercury	1
HD 179949 b	Confirmed	288.8875, −24.1792	Venus	1
HD 204313 b,c,d	Confirmed	322.0500, −21.7264	Mercury	1
HD 212771 b	Confirmed	336.7625, −17.2636	Mercury	1
HD 222582 b	Confirmed	355.4625, −5.9856	Venus	1
HD 283668 b	Confirmed	66.9708, 24.4447	Mercury	1
HD 284149 b	Confirmed	61.6625, 20.3031	Venus	1
HD 32963 b	Confirmed	76.9833, 26.3281	Mercury	1
HD 5319 b,c	Confirmed	13.7542, 0.7894	Mercury	1
HD 62509 b	Confirmed	116.3250, 28.0261	Mercury	1
HD 79498 b	Confirmed	138.7875, 23.3756	Mercury	1
HD 88133 b	Confirmed	152.5292, 18.1867	Mercury	1
HD 89307 b	Confirmed	154.5875, 12.6208	Mars	1
HIP 78530 b	Confirmed	240.4792, −21.9803	Mercury	1
K2-14 b	Confirmed	178.0570, 2.5942	Mars	1
K2-15 b	Confirmed	178.1108, 4.2547	Venus	1
K2-17 b	Confirmed	178.3298, 6.4123	Mercury	1
K2-31 b	Confirmed	245.4408, −23.5479	Mercury	1
LKCA 15 b	Confirmed	69.8250, 22.3508	Earth	1
MOA-2011-BLG-293L b	Confirmed	268.9125, −28.4769	Mercury	1
MOA-2013-BLG-220L b	Confirmed	270.9875, −28.4553	Mercury	1
OGLE-2011-BLG-0251L b	Confirmed	264.5591, −27.1361	Mercury	1
OGLE-2012-BLG-0026L b,c	Confirmed	263.5792, −27.1428	Mercury	1
OGLE-2012-BLG-0358L b	Confirmed	265.6958, −24.2611	Venus	1
OGLE-2012-BLG-0563L b	Confirmed	271.4905, −27.7120	Mercury	1
OGLE-2013-BLG-0723L B b	Unconfirmed	263.6708, −27.4481	Mercury	1
OGLE-2014-BLG-0124L b	Confirmed	270.6208, −28.3964	Mercury	1
OGLE-2014-BLG-0257L b	Confirmed	270.4500, −28.2619	Mercury	1
OGLE-2015-BLG-0051L b	Confirmed	269.6625, −28.0317	Mercury	1
OGLE-2015-BLG-0954L b	Confirmed	270.1833, −28.6608	Mercury	1
Pr 0201 b	Confirmed	130.4333, 20.2269	Mars	1
ROXs 12 b	Confirmed	246.6042, −24.5433	Mercury	1
ROXs 42B b	Confirmed	247.8125, −24.5456	Mercury	1
SR 12 AB c	Confirmed	246.8333, −24.6944	Mercury	1
V830 Tau b	Confirmed	68.2917, 24.5619	Mercury	1
WASP-157 b	Confirmed	201.6542, −8.3175	Mars	1
WASP-47 b,c,d,e	Confirmed	331.2042, −12.0189	Earth	1
WASP-68 b	Confirmed	305.0958, −19.3147	Earth	1
WD 1145+017 b	Confirmed	177.1375, 1.4831	Earth	1

This paper has been typeset from a TEX/LATEX file prepared by the author.